Magnetic hyperfine interactions on Cd sites of the rare-earth cadmium compounds *R*Cd (*R*=Ce, Pr, Nd, Sm, Gd, Tb, Dy, Ho, and Er)

F. H. M. Cavalcante
Instituto de Pesquisas Energéticas e Nucleares - IPEN/CNEN, Universidade de São Paulo, São Paulo, SP, Brazil and Department of Electrical and Computer Engineering at Colorado State University, Fort Collins, Colorado, USA

O. F. L. S. Leite Neto*
Centro Brasileiro de Pesquisas Físicas - CBPF/MCTI, Rio de Janeiro, Brazil and Instituto de Engenharia Nuclear - IEN/CNEN, Rio de Janeiro, Brazil

H. Saitovitch and J. T. P. D. Cavalcante
Centro Brasileiro de Pesquisas Físicas - CBPF/MCTI, Rio de Janeiro, Brazil

A. W. Carbonari,† R. N. Saxena, B. Bosch-Santos, L. F. D. Pereira, and J. Mestnik-Filho
Instituto de Pesquisas Energéticas e Nucleares - IPEN/CNEN, Universidade de São Paulo, São Paulo, SP, Brazil

M. Forker
Centro Brasileiro de Pesquisas Físicas - CBPF/MCTI, Rio de Janeiro, Brazil and Helmholtz Institut für Strahlen- und Kernphysik - Universität Bonn, Bonn, Germany
(Received 1 April 2016; revised manuscript received 26 July 2016; published 15 August 2016)

This paper reports the investigation of the magnetic hyperfine field B_{hf} in a series of rare-earth (R) cadmium intermetallic compounds RCd and $GdCd_2$ measured by perturbed angular correlation (PAC) spectroscopy using ^{111}In/^{111}Cd as probe nuclei at Cd sites as well as first-principles calculations of B_{hf} at Cd sites in the studied compounds. Vapor–solid state reaction of R metals with Cd vapor and the ^{111}In radioisotope was found to be an appropriate route of doping rare-earth cadmium compounds with the PAC probe ^{111}In/^{111}Cd. The observation that the hyperfine parameters depend on details of the sample preparation provides information on the phase preference of diffusing ^{111}In in the rare-earth cadmium phase system. The ^{111}Cd hyperfine field has been determined in the compounds RCd for the R constituents Ce, Pr, Nd, Sm, Gd, Tb, Dy, Ho, and Er, in several cases as a function of temperature. For most R constituents, the temperature dependence $B_{hf}(T)$ of ^{111}Cd:RCd is consistent with ferromagnetic order of the compound. DyCd, however, presents a remarkable anomaly: a finite magnetic hyperfine field is observed only in the temperature interval $35\ \mathrm{K} \leqslant T \leqslant 80\ \mathrm{K}$ which indicates a transition from ferromagnetic order to a spin arrangement where all $4f$-induced contributions to the magnetic hyperfine field at the Cd site cancel. First-principles calculation results for DyCd show that the $(\pi, \pi, 0)$ antiferromagnetic configuration is energetically more favorable than the ferromagnetic. The approach used in the calculations to simulate the RCd system successfully reproduces the experimental values of B_{hf} at Cd sites and shows that the main contribution to B_{hf} comes from the valence electron polarization. The de Gennes plot of the hyperfine field B_{hf} of ^{111}Cd:RCd vs the $4f$-spin projection $(g-1)J$ reflects a decrease of the strength of indirect $4f$-$4f$ exchange across the R series. Possible mechanisms are discussed and the experimental results indicate that the indirect coupling is provided by the intra-atomic $4f$-$5d$ exchange and interatomic $5d$-$5d$ interaction between the spin-polarized $5d$ electrons of neighboring R atoms. The ratio of the hyperfine fields of GdCd and $GdCd_2$ scales with the number of nearest Gd neighbors. In the paramagnetic phases of the RCd compounds, the PAC spectra indicate the presence of a broad distribution of weak quadrupole interactions suggesting a perturbation of the cubic CsCl symmetry of the Cd site, most probably due to chemical disorder of the R and Cd sublattices. A substantial interchange of R and Cd atoms is also reflected in the temperature dependence of the linewidth of the magnetic hyperfine interaction in the magnetically ordered phase of RCd and $GdCd_2$. Its critical increase towards the order temperature is evidence for a distribution of the order temperature with a width of about 10 K.

DOI: 10.1103/PhysRevB.94.064417

I. INTRODUCTION

Measurements of magnetic and electric hyperfine interactions (HFIs) of magnetically ordered compounds [1] may provide information on the exchange interactions leading to spontaneous magnetic order, on the order of magnetic phase transitions, on spin wave excitations, on relaxation processes, and on other parameters characterizing a magnetic system.

Much of the experimental and theoretical hyperfine interaction work has been focused on magnetic systems involving the rare-earth (R) elements Ce to Tm. As these elements differ in the number of well-shielded $4f$ electrons, they have rather

*Current address: Instituto de Pesquisas Energéticas e Nucleares - IPEN/CNEN, Universidade de São Paulo, São Paulo, SP, Brazil.
†carbonar@ipen.br

similar chemical properties. The $4f$ spins play a decisive role in the exchange interactions. The orbital contributions to the $4f$ magnetic moments, however, vary strongly with the number of $4f$ electrons. Consequently, one finds a large number of isostructural series of R compounds [2,3] that—for different R constituents—differ only slightly in the crystallographic properties, but strongly in the magnetic properties and thus offer favorable conditions for the separation of the magnetic from other solid-state parameters.

In the large group of magnetic binary rare-earth intermetallics the most frequently occurring compositions are RX and RX_2. Many of these intermetallics have been investigated by measuring the HFIs mostly of the non-rare-earth constituents or of impurity nuclei. At R nuclei (except Gd), magnetic fields and electric field gradients (EFGs) are predicted to be very large [4], caused by the unquenched orbital angular momentum of the $4f$ shell and the asphericity of external electronic shells, respectively. Consequently, a precise determination of the much smaller contributions to the hyperfine interaction produced by the magnetic host may become difficult.

Among the equiatomic RX, those with the nonmagnetic constituents X = Cu, Ag, Rh, Zn, Mg, Cd, and Hg crystallize in the cubic CsCl structure [5]. This group appears attractive for magnetic HFI studies: Because of the cubic symmetry one expects no quadrupole interaction on the RX lattice sites and one may therefore anticipate a simple HFI situation, with the only contribution coming from the magnetic hyperfine field B_{hf}. The few HFI studies of RX compounds with CsCl-type structure reported up to now are mainly limited to GdX, X = Cd, Zn. The hyperfine fields of impurity nuclei on X sites [6,7] and of constituent nuclei [8] of these compounds were investigated by the NMR technique, with the experimental trends discussed by de Oliveira *et al.* [9] in the framework of a two-center model.

The experimental information on the effect of the R constituent on impurity hyperfine fields in RX compounds is scarce: ^{119}Sn Moessbauer [10] and ^{111}Cd perturbed angular correlation (PAC) spectroscopy [11–13] have been applied to some RZn, mainly with heavy R constituents. The variation of B_{hf} for a given impurity across the entire R series from Ce to Tm has still to be established. This question is addressed in the present paper which reports a PAC study of the HFI of the nuclear probe ^{111}Cd in RCd for the R constituents R = Ce, Pr, Nd, Sm, Gd, Tb, Dy, Ho, Er. For the interpretation of unexpected features of the PAC spectra of some RCd compounds, the investigation was extended to the HFI of ^{111}Cd in the trigonal $CeCd_2$-type compound $GdCd_2$ [14–17].

The properties of equiatomic RX compounds have been studied in detail by x-ray diffraction [18,19], magnetization measurements [18,20,21], and resistivity [22,23]. Magnetic susceptibility [24] was used to detect structural phase transitions. The members of the RCd series with the heavy R constituents R = Gd, Dy, Tb, Ho, and Er have been reported to be ferromagnetic [18,20]. According to Fuji *et al.* [25], the members with the light R = Nd and Ce also order ferromagnetically whereas in Ref. [22] CeCd is mentioned as antiferromagnetic. PrCd exhibits metamagnetic behavior in the magnetization curve and can be understood as an antiferromagnet in zero magnetic field [18,26]. According to Buschow [20], SmCd is ferromagnetic with T_C = 190 K, whereas Alfieri *et al.* [18] have concluded from magnetization measurements that this compound is diamagnetic at low temperature and becomes paramagnetic at 110 K.

In the work reported in this paper the magnetism in the compounds RCd, where R = Ce, Pr, Nd, Sm, Gd, Tb, Dy, Ho, Er, were investigated by measuring the magnetic hyperfine field (B_{hf}) at Cd sites using ^{111}Cd as probe nuclei as well as by *ab initio* calculations based on density functional theory (DFT). Since neutron diffraction measurements of these compounds are difficult to perform due to the very large neutron absorption cross section of Cd and most of rare-earth elements, an atomic view on the magnetism of this series of compounds is probably only possible through the investigation of hyperfine interactions. First, we describe and discuss the method used to prepare the samples, which are quite difficult to obtain due to the low vapor pressure of rare-earth elements and the low melting temperature of Cd, and the way to introduce the ^{111}In(^{111}Cd) probes, which was only successfully achieved by melting them along with the constituent elements of the compounds. We show that thermal diffusion of probe nuclei did not succeed because of the additional annealing at high temperature. Most likely, ion implantation of radioactive probes will not succeed as well because of the necessity of additional annealing to recover the local structure. Second, from the unprecedented experimental results for the magnetic hyperfine field at Cd sites in almost the complete series of RCd compounds, it was possible to discuss the origin of the magnetic exchange mechanism between rare-earth ions, which was found to be a direct d-d interatomic coupling polarized by an f-d intra-atomic interaction. This conclusion does not agree with the previously reported work [20] that claimed that the main magnetic coupling mechanism is the RKKY [27] but suggested the presence of a second mechanism. Third, from values of B_{hf} obtained from *ab initio* calculations, which unexpectedly agree quite well with the experimental ones, it was possible to determine the main contribution to B_{hf} and also determine the origin of the so far not understood magnetic transition at 40 K observed in DyCd. Moreover, the successful calculation method described in this paper consists of a recipe for future calculations in similar compounds. Finally, from the temperature dependence of experimental B_{hf} it was possible to investigate the distribution of the magnetic order temperature and quantitatively determine the linewidths of the T_C distribution of the compounds. Furthermore, understanding the magnetism in the compounds of the RCd basic series is a fundamental starting point to investigate the magnetism in complex compounds with rare-earth elements and cadmium such as the new icosahedral binary quasicrystals formed by rare-earth elements and cadmium in which the nature of magnetic transitions in aperiodic lattices is not understood yet [28].

II. EXPERIMENTAL DETAILS

A. Sample preparation and equipment

The PAC measurements were carried out with the 173–247 keV $\gamma\gamma$ cascade of ^{111}Cd which is populated in the electron capture decay of the 2.8 d isotope ^{111}In. The compounds

to be investigated by PAC have therefore to be doped with radioactive ^{111}In which is commercially available as a dilute solution of $^{111}InCl_3$ in HCl. Because of the high vapor pressure of Cd, rare-earth cadmium compounds are usually prepared using vapor–solid state reactions by heating the metallic constituents—sealed in Ta or Mo containers—for several hours at temperatures of about 1250 K. In the present study Ta containers enclosed in evacuated quartz tubes were used. X-ray diffraction of the reaction products confirmed the cubic CsCl structure plus—in some cases—a small contamination by nonreacted Cd metal. Reflections coming from nonreacted rare-earth metal and other *R*-Cd compounds were not observed.

Two procedures for doping with radioactive ^{111}In were tested: (i) doping subsequent to synthesis and (ii) simultaneous doping during synthesis. In the first procedure, $^{111}InCl_3$ was deposited onto the ready *R*Cd compounds, which were then encapsulated under vacuum in quartz tubes and heated at 1200 K for about 12 hours. For simultaneous doping during synthesis, $^{111}InCl_3$ was added to the metallic constituents brought to reaction in the Ta container. These two procedures were found to produce marked differences in the HFI parameters, indicating that for the same nominal composition different doping conditions may result in different local environments of the probe nuclei. For an understanding of these differences, the study was extended to the *R*-Cd intermetallic $GdCd_2$, synthesized and simultaneously doped by vapor–solid state reaction of the constituents.

The PAC measurements were carried out with a standard PAC setup equipped with four BaF_2 detectors. For temperature variation two closed-cycle He refrigerators were used, initially one reaching 15 K; later another one attaining 4.0 K became available. In the case of ErCd ($T_C = 3.3$ K) a pumped bath of liquid helium was used to cool the sample down to 2 K.

B. Data analysis

The angular correlation theory of two successive γ rays of a $\gamma\gamma$ cascade, expressed by angular correlation coefficients A_{kk} ($k = 2,4$), may be modulated in time by hyperfine interactions in the intermediate state of the cascade. For polycrystalline samples this modulation can be described by the perturbation factor $G_{kk}(t)$ which depends on the multipole order, the symmetry and time dependence of the interaction, and the spin of the intermediate state (for details see, e.g., Frauenfelder and Steffen [29]).

For static hyperfine interactions in polycrystalline samples the perturbation factor can be written as a sum of oscillatory terms:

$$G_{kk} = s_{k0} + \sum_n S_{kn} \cos(\omega_n t). \tag{1}$$

The frequencies ω_n are related to the energy differences between the hyperfine levels into which a nuclear state is split by the hyperfine interaction. In the most general case of a combined magnetic and electric HFI, these frequencies and the amplitudes s_{kn} have to be determined by diagonalization of the interaction Hamiltonian. In the most general case, there are five HFI parameters [30]: (i) the magnetic interaction frequency $\nu_m = g\mu_N B_{hf}/h$, where g is the g factor of the nuclear state under consideration, μ_N the nuclear magneton, and B_{hf} the magnetic hyperfine field; (ii) the quadrupole frequency $\nu_q = eQV_{zz}/h$, with Q the nuclear quadrupole moment and V_{zz} the maximum component of the EFG tensor; (iii) the asymmetry parameters of the EFG tensor $\eta = (V_{xx} - V_{yy})/V_{zz}$; and (iv) and (v) the Euler angles β, γ describing the orientation of B_{hf} in the principal-axes system of the EFG tensor. The number of terms in Eq. (1) depends on the spin I of the intermediate state. In the present paper we are dealing mainly with the perturbation by a pure magnetic interaction with Larmor frequency $\omega_m = 2\pi\nu_m$. In this situation, the perturbation factor can be expressed analytically as

$$G_{22}(t) = 1/5 + 2/5 \sum_{n=1,2} \cos(n\omega_m t). \tag{2}$$

If the ensemble of the probe nuclei is subject to a distribution rather than a unique hyperfine interaction, the nuclear spins of the ensemble no longer precess all with the same frequency resulting in an attenuation of the oscillation amplitudes, which is stronger when the distribution is broader. The effect of a Lorentzian HFI distribution of relative width δ on the angular correlation can be approximated by

$$G_{kk}(t) = s_{k0} + \sum_n S_{kn} \cos(\omega_n t) \exp(-\delta_n \omega_n t). \tag{3}$$

Frequently, several fractions of nuclei subject to different HFIs are found in the same sample. The effective perturbation factor is then given by

$$G_{kk}(t) = \sum_i f_i G^i_{kk}(t), \tag{4}$$

where f_i (with $\sum_i f_i = 1$) is the relative intensity of the ith fraction.

III. MEASUREMENTS AND RESULTS

The ^{111}Cd PAC spectra of nominally equiatomic *R*Cd compounds were found to depend sensitively on the doping procedure used to introduce the radioactive mother isotope ^{111}In. Doping "subsequent to synthesis" by diffusing ^{111}In into ready GdCd compounds resulted in spectra (see left-hand panels of Fig. 1 and Fig. 2) characterized by an axially symmetric quadrupole interaction (QI) at room temperature. Upon cooling, a combined magnetic and electric HFI set evidence for the onset of magnetic order. At 4 K the parameters of this combined interaction are $\nu_m = 59$ MHz, $\nu_q = 200$ MHz, $\eta = 0$, and $\beta \sim 120°$.

The observation of a finite QI and of a magnetic perturbation at $T \leqslant 85$ K is incompatible with the cubic CsCl structure and the magnetic properties of GdCd (magnetic order temperature $T_C \sim 265$ K [5]). Clearly, the nuclear probes—when diffused into the ready compound—do not end up on lattice sites of equiatomic GdCd, but of some other Gd-Cd compound of noncubic symmetry and an order temperature of ~85 K. These properties suggest that trigonal $GdCd_2$ might be the compound in question. The Curie temperature of $GdCd_2$ has not yet been reported, but that of the related compound $GdZn_2$ ($T_C \sim 70$ K [31]) is rather close to the order temperature seen in Fig. 1. For an experimental test of this conjecture, PAC spectra of ^{111}Cd in $GdCd_2$ were taken at different temperatures (right-hand panel of Fig. 2). Figure 3 compares the ^{111}Cd

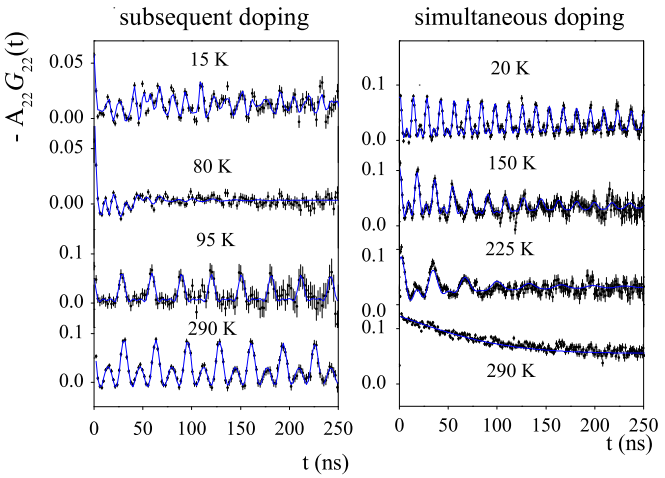

FIG. 1. PAC spectra of ^{111}Cd in a Gd-Cd compound with nominal composition 1:1 prepared by vapor–solid state reaction of the constituents in a Ta container at 1250 K. The two panels illustrate the influence of the doping procedure on the HFI parameters: The spectra of the left-hand panel were observed when the PAC mother isotope ^{111}In was introduced into the ready reaction product by subsequent diffusion at 1000 K for 24 h. The right-hand panel shows spectra obtained when the compound was doped during synthesis by adding $^{111}InCl_3$ to the metallic constituents brought to reaction in a Ta container.

HFI parameters of CdGd "simultaneously doped" during synthesis (full black squares) and GdCd doped "subsequent to synthesis" (full blue squares) to those of $GdCd_2$ (full red squares). The perfect agreement of the blue (GdCd) and red ($GdCd_2$) sets of parameters in Fig. 3 is clear evidence for the formation of ^{111}Cd:$GdCd_2$ in a compound of GdCd doped with

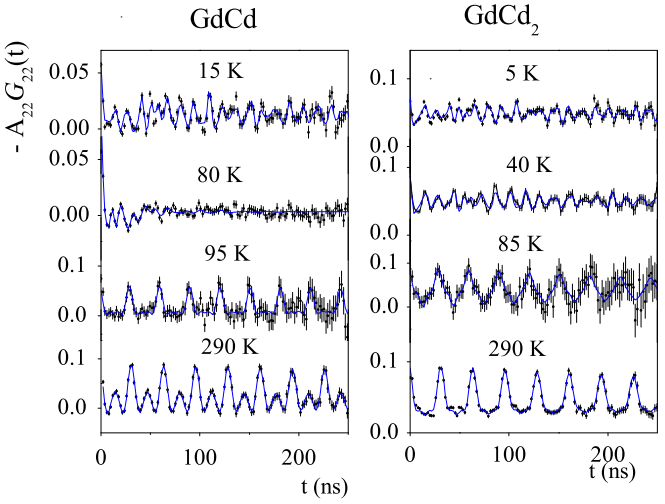

FIG. 2. PAC spectra of ^{111}Cd in compounds of Gd-Cd system. The left-hand panel shows spectra of a Gd-Cd compound with nominal composition 1:1 prepared by vapor–solid state reaction of the constituents at 1250 K. In this case the PAC nucleus was introduced in the reaction product by subsequent diffusion of ^{111}In at 1000 K for 24 h. The spectra of the right-hand panel were obtained with a compound of nominal composition 1:2, simultaneously doped during synthesis.

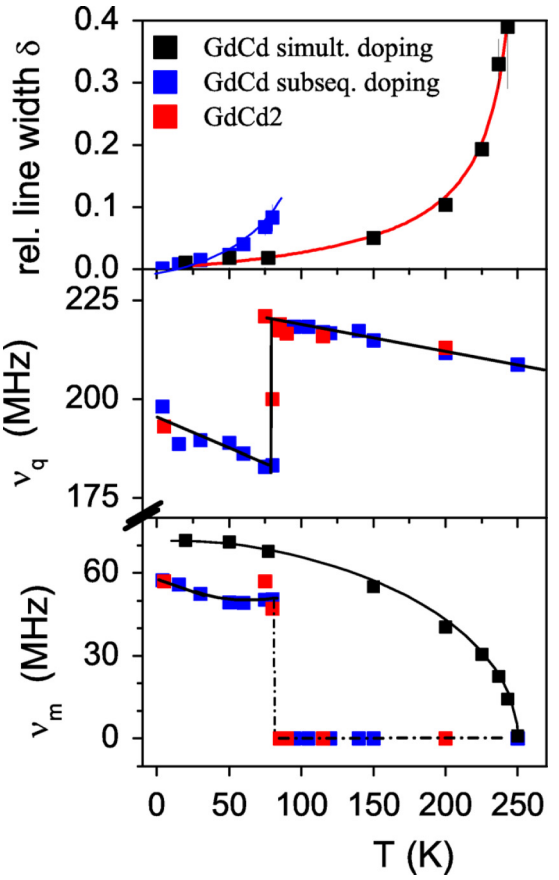

FIG. 3. The magnetic hyperfine frequency ν_m, the quadrupole frequency ν_q, and the relative width δ of the magnetic frequency distribution extracted from the spectra of ^{111}Cd:GdCd in the left-hand panel (blue squares) and the right-hand panel (black squares) of Fig. 1, respectively. The full red squares in the bottom and middle sections correspond to the frequencies ν_m and ν_q extracted from the spectra of ^{111}Cd:$GdCd_2$ (right-hand panel of Fig. 2), respectively. The red line in the topmost section shows a fit of Eq. (6) to the relative linewidth δ (black squares) of the magnetic frequency distribution. The solid line in the bottom section is the result of a fit of the molecular-field model for spin 7/2 to the magnetic frequencies.

^{111}In subsequent to synthesis. In the x-ray pattern of GdCd, reflections of other Gd-Cd phases were below the limit of detection. The observation of PAC spectra incompatible with GdCd then implies that in a *R*-Cd phase mixture diffusing ^{111}In prefers other *R*-Cd phases—in the present case trigonal RGd_2—over cubic *R*Cd, even if those phases are present only in minuscule quantities. A similar observation has been reported for *R*-Ga intermetallics where ^{111}In was found to strongly prefer RGa_2 over *R*Ga [32,33]. The second doping procedure, where $^{111}InCl_3$ is added to the metallic constituents to be reacted, led to HFI parameters compatible with the cubic CsCl structure ($\nu_q = 0$) and the known magnetic properties of GdCd (full black squares in the lowest section of Fig. 3). The investigation of the *R* dependence of the HFI parameters in *R*Cd was therefore carried out with compounds doped simultaneously during synthesis. Figures 4, 5, and 6 show the ^{111}Cd spectra of NdCd, DyCd, and TbCd, respectively, recorded under these conditions.

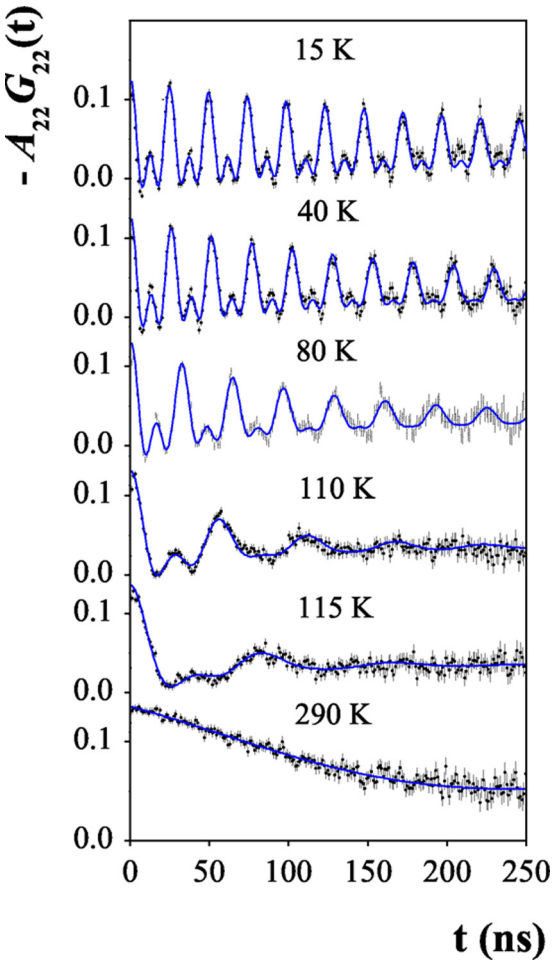

FIG. 4. PAC spectra of ^{111}Cd in NdCd at different temperatures. For sample preparation the metallic constituents were sealed—together with radioactive $^{111}InCl_3$—in a Ta tube under argon atmosphere and heated to 1250 K for 10 hours.

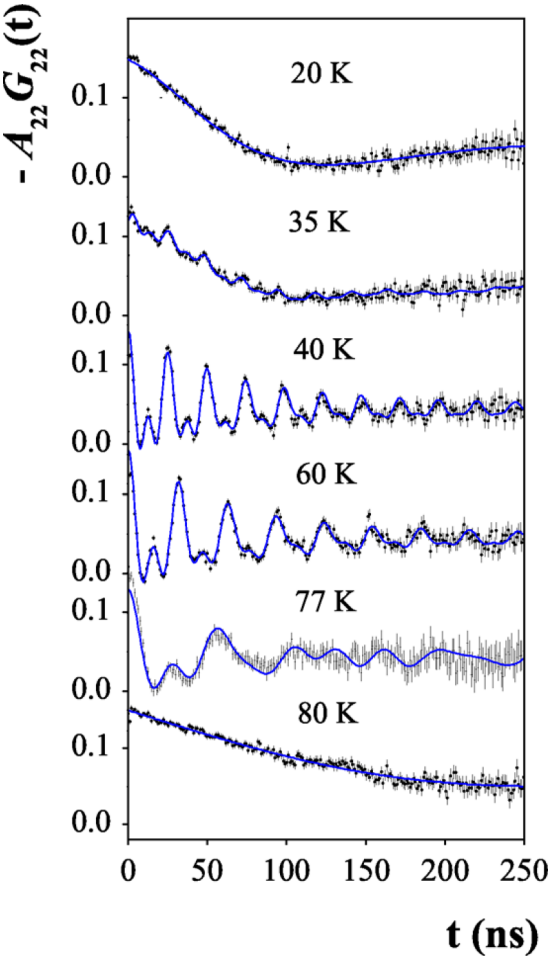

FIG. 5. PAC spectra of ^{111}Cd in DyCd at different temperatures.

At the lowest temperature of 15 K used in the measurement of NdCd, one observes a fast, practically periodic modulation of the anisotropy reflecting the spin precession caused by a magnetic hyperfine interaction. The period of precession increases with temperature. The magnetic interaction disappears at $T \sim 120$ K, giving way to a perturbation by a weak QI distribution. The spectra of the other *R*Cd compounds produced by simultaneous doping present the same characteristics.

An interesting feature of the spectra in Figs. 4, 5, and 6 is the attenuation of the oscillation amplitude with time in the magnetic phases and the fact that this attenuation strongly increases with increasing temperature. In principle, such attenuation may be attributed either to the presence of a weak quadrupole interaction, as proposed for the similar case of ^{111}Cd in the cubic CsCl compounds *R*Zn [11–13], or to a finite distribution of the magnetic hyperfine field.

The description of the attenuation of the 15 K spectrum of ^{111}Cd:NdCd by a combined magnetic and electric interaction would require a quadruple frequency of $\nu_q \sim 2.5$ MHz (assuming an axially symmetric EFG and $\beta = 0$ for the angle between the EFG and B_{hf}) and the increase of the attenuation towards higher temperatures would correspond to an increase to $\nu_q \sim 7$ MHz at 110 K. To account for a finite QI either at the Cd or Gd sites of cubic GdCd, the cubic CsCl symmetry would have to be broken by, e.g., the presence of some kind of defect. Defects caused by chemical disorder (Cd on Gd sites, Gd on Cd sites) are probably present, but one would not expect that the corresponding QI strongly increases with increasing temperature. In metallic systems the QI usually decreases towards higher T [34].

We therefore attribute the attenuation of the oscillation amplitudes to a distribution of the magnetic hyperfine frequency ν_m. Consequently, the spectra of *R*Cd, $R =$ Nd, Sm, Gd, and Dy, were analyzed by fitting the perturbation function for pure magnetic HFIs [Eq. (3)] to the experimental data. It was assumed that the Larmor frequency ν_m presents a Lorentzian distribution of relative width δ. The results of the analysis for *R*Cd; $R =$ Nd, Sm, and Gd, are collected in Fig. 7.

The spectra of ^{111}Cd:DyCd (Fig. 5) are also characterized by a pure magnetic interaction, but in contrast to *R*Cd, $R =$ Nd, Sm, and Gd, two magnetic transitions are observed: A magnetic interaction appears discontinuously only at $T \sim 35$ K. At lower temperatures the spectra show no magnetic precession. At $T > 35$ K, the magnetic frequency decreases with increasing temperature towards $T_C \sim 80$ K. In the magnetic region of DyCd the relative linewidth δ of the

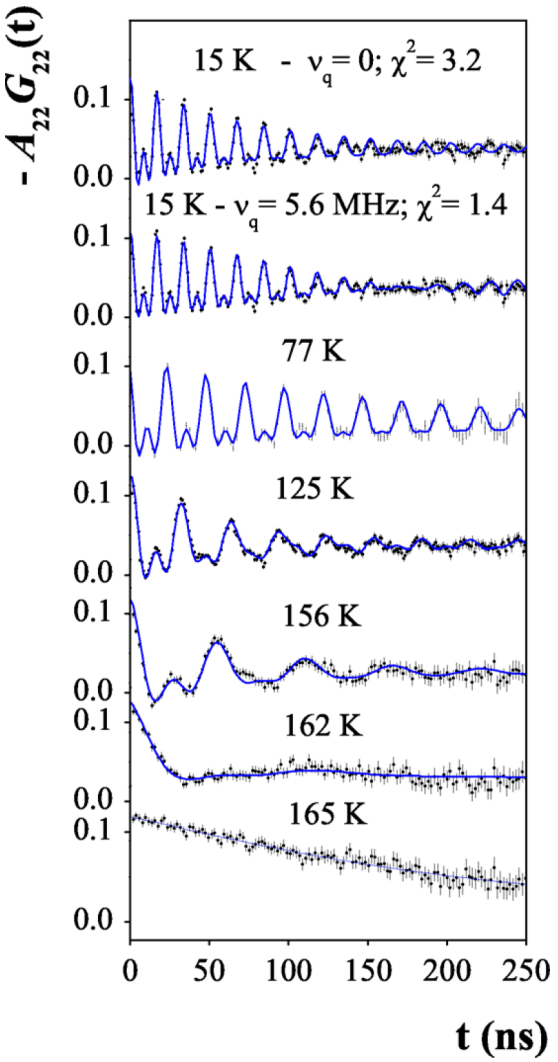

FIG. 6. PAC spectra of ^{111}Cd in TbCd at different temperatures. The topmost sections show two different fits of the spectrum measured at 15 K, one attributing the attenuation of oscillation amplitudes to a distribution of the magnetic hyperfine field, the other allowing for the presence of a finite quadrupole interaction.

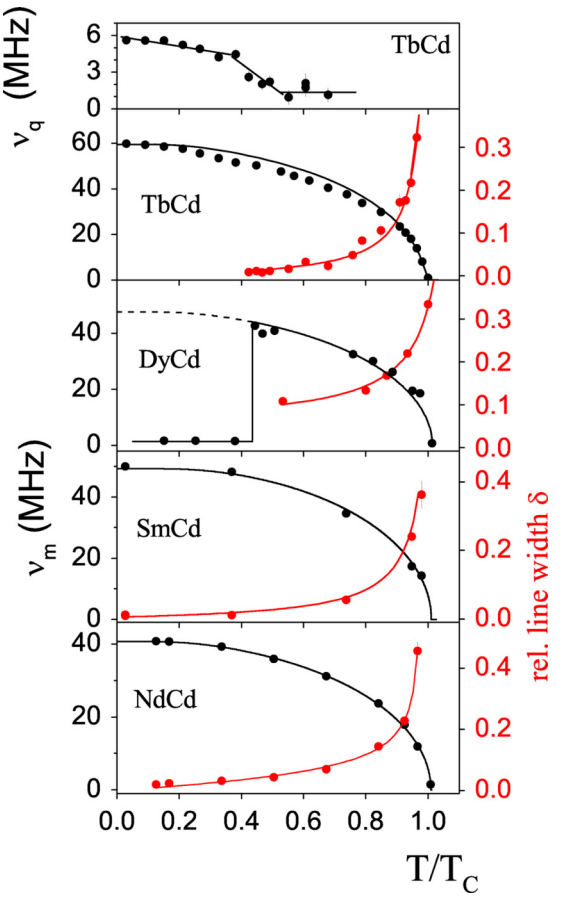

FIG. 7. The temperature dependence of the magnetic interaction frequency ν_m (black points) and the relative width δ of its distribution (red points) of ^{111}Cd in NdCd, SmCd, DyCd, and TbCd. The black lines are the Brillouin functions for the corresponding angular momentum J and the red lines represent fits of Eq. (6) to the relative linewidths δ of the magnetic field distribution. The topmost section shows the temperature dependence of the quadrupole interaction detected in the spectra of TbCd.

magnetic frequency increases critically towards the order temperature, just as in the other *R*Cd compounds.

Figure 6 shows the PAC spectra of ^{111}Cd in TbCd. This is the only compound in the *R*Cd series, for which we found evidence of a well defined quadrupole interaction at $T < 65$ K; the amplitude modulation at times $t < 150$ ns in the 15 K spectrum of TbCd is much better reproduced by the assumption of a combined magnetic and electric HFI (second section from top in Fig. 6; reduced $\chi^2 \sim 1.4$) than by a Lorentz distribution of pure magnetic interaction (topmost section in Fig. 6; reduced $\chi^2 \sim 3.2$). Furthermore, the damping of the oscillation amplitudes strongly decreases from 15 K to 77 K and then increases again towards higher temperatures. In the case of a pure magnetic HFI this trend would imply that the width of the magnetic frequency distribution passes through a minimum at $T \sim 77$ K. The spectra of TbCd were therefore analyzed assuming a combined interaction with $\eta = 0$, $\beta = 0$.

The HFI parameters ν_m and δ of ^{111}Cd in *R*Cd, R = Nd, Sm, Dy, and Tb, derived from the spectra in Figs. 4, 5, and 6, are collected in Fig. 7. The top section of this figure shows the temperature dependence of the quadrupole frequency ν_q of ^{111}Cd:CdTb.

Low-temperature PAC spectra of the compounds *R*Cd, R = Ho, Er, Pr, and Ce, are collected in Fig. 8. In the case of HoCd, the data suggest the presence of two hyperfine fields of comparable intensity (ν_m = 19.7 MHz and 22.7 MHz, respectively, at 9 K; red lines in Fig. 8). ErCd was found to be paramagnetic at 4 K. When immersed into a pumped bath of liquid He at 2 K, a magnetic precession with ν_m = 16.1 MHz was observed. Metamagnetic PrCd showed no magnetic precession at T = 10 K, consistent with its antiferromagnetic structure in zero magnetic field [18,26]. At $T < 16$ K CeCd presented a weak, strongly distributed magnetic interaction centered at $\nu_m \sim 5$ MHz.

The main experimental results of the present investigation for $\nu_m(0)$, $B_{hf}(0)$, and T_C are listed in Table I.

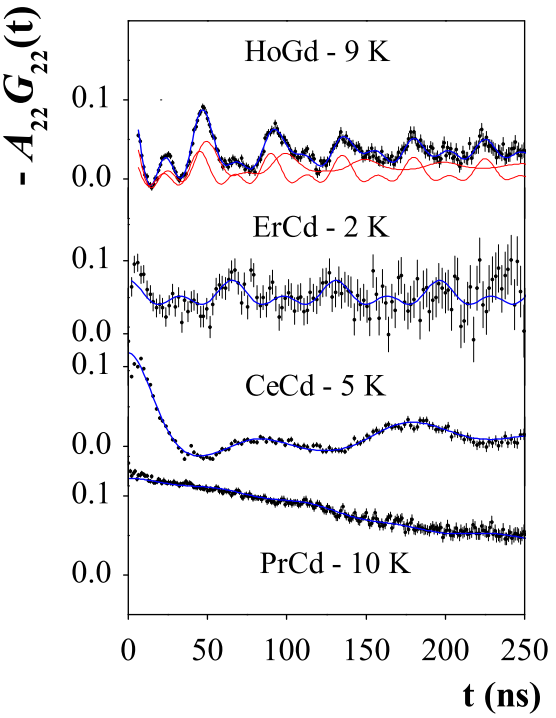

FIG. 8. PAC spectra of ^{111}Cd in *R*Cd, *R* = Ho, Er, Pr, Ce at low temperatures. In the case of HoCd, two fractions with slightly different frequencies (red lines) are needed for the description of the experimental data.

IV. DISCUSSION

A. The magnetic hyperfine field: Spin and temperature dependence

In Table I our experimental saturation values of B_{hf} of ^{111}Cd in *R*Cd are compared with the results of ^{111}Cd [11] and ^{119}Sn [10] in some *R*Zn compounds. For ^{111}Cd in RX, B_{hf} is practically independent of the X constituent and the probe dependence of B_{hf} in *R*Zn is also very weak. Our PAC result for the hyperfine field of ^{111}Cd in GdCd (B_{hf} = 30.8 T) is in fair agreement with the NMR result (B_{hf}= 31.8 T) of Kasamatsu *et al.* [6,8].

Because of the small radial extension of the $4f$ electrons, magnetic order in rare-earth compounds requires a mechanism of indirect exchange between the $4f$ electrons. Mainly two mechanisms of indirect $4f$-$4f$ coupling have been proposed: In the Ruderman-Kittel-Kasuya-Yosida (RKKY) theory [27] the coupling is mediated by the s-conduction electrons, which are spin polarized by exchange with the $4f$ electrons. In an alternative concept, which was proposed by Campbell [35], the indirect coupling is provided by intra-atomic $4f$-$5d$ exchange and interatomic $5d$-$5d$ interaction between the spin-polarized $5d$ electrons of neighboring R atoms. Since the $5d$ electrons are strongly more localized than the s electrons, one would expect that the hyperfine field is mainly determined by the number N and the separation R_{NN} of the nearest R neighbors.

In both concepts the spin polarization leads, via the Fermi contact term in the nucleus-electron interaction, to a magnetic hyperfine field B_{hf} at the nuclei of non-rare-earth atoms. The spin polarization is expected to be proportional to the $4f$ spin projection $(g-1)J$ and the exchange parameter Γ of the concept in question (for details see, e.g., [36]). The hyperfine field can then be written

$$B_{hf} \propto C\Gamma(g-1)J\Phi(r). \tag{5}$$

In the RKKY coupling, the function $\Phi(r)$ is given by the sum $\Phi(r)|_{f-f} = \sum_{n\neq m} F(2k_F R_{nm})$ over all R constituents, with $F(x) = (\sin x - x\cos x)/x^4$ corresponding to the oscillating RKKY range function. For dominant $4f$-$5d$ and $5d$-$5d$ coupling, one would have $\Phi(r)|_{f-d} = \sum_{i=1}^{N} f(R_i)$, with the sum extending over the N nearest R neighbors of the probe and $f(R_i)$ describing the radial dependence of the exchange. The parameter C in Eq. (5) accounts—in the case of impurity probes—for the modification of the host's s-electron

TABLE I. The saturation value of the magnetic hyperfine frequency $\nu_m(0)$ and the corresponding magnetic hyperfine field $B_{hf}(0)$ at ^{111}Cd in *R*Cd determined from the low-temperature PAC spectra. In the case of DyCd the saturation value was estimated by using the molecular field model to extrapolate the experimental trend of $\nu_m(T \leqslant 35\ \text{K})$ to $T = 0$. T_C is the value of the order temperature derived from the temperature dependence of the magnetic frequency. Values of B_{hf} at probe nuclei ^{111}Cd and ^{119}Sn in equiatomic *R*Zn for some *R* constituents [10,11] are included.

	Rare-earth properties			^{111}Cd:*R*Cd this work		^{111}Cd:*R*Zn Ref. [11]	^{119}Sn:*R*Zn Ref. [10]
R	$(g-1)J$	$(g-1)^2J(J+1)$	T_C (K)	$\nu_m(0)$ (MHz)	$B_{hf}(0)$ (T)	$B_{hf}(0)$ (T)	$B_{hf}(0)$ (T)
Ce	−0.36	0.179	15	12	5.1		
Pr	−0.80	0.800					
Nd	−1.23	1.841	119	40.7	17.4		
Sm	−1.79	3.200	190	49.3	21.1		23.4
Gd	3.50	15.750	247	71.8	30.8	32	35.5
Tb	3.00	10.500	163	59.7	25.6	26.4	27.9
Dy	2.50	7.069	79	46.7	20.0	19.7	20.9
Ho I	2.00	4.500	15.5	24	10.3		13.1
Ho II	2.00	4.500	15.5	26	11.1		
Er	1.50	2.550	3	16.1	6.9		

spin polarization by spin-dependent electron scattering at the impurity potential [37].

As discussed in Ref. [11], the comparison of the hyperfine field of ^{111}Cd in *R*Zn compounds to that in *R* metals suggests that $4f$-$5d$ exchange and $5d$-$5d$ interaction plays the dominant role in the indirect *R*-*R* coupling of *RX*, *X* = Cd, Zn. This conclusion is also supported by the difference of the magnetic hyperfine fields of ^{111}Cd in GdCd ($B_{hf} = 30.8$ T) and $GdCd_2$ ($B_{hf} = 25$ T), respectively: The Cd site of GdCd has 8 nearest Gd neighbors (*nn*) at 3.25 Å; in the case of $GdCd_2$ there are 3 *nn* Gd at 3.22 Å and 3 *nn* Gd at 3.47 Å. Since the Cd-Gd distances in GdCd and $GdCd_2$ differ only slightly, the concept of $4f$-$5d$ exchange and $5d$-$5d$ interaction predicts a hyperfine field ratio of $B_{hf}(GdCd_2)/B_{hf}(GdCd) \sim 6/8 = 0.75$, fairly close to the experimental ratio of $25/30.8 = 0.8$.

Whatever the coupling scheme, according Eq. (5) the variation of B_{hf} for a series of isostructural rare-earth compounds reflects the *R* dependence of the relevant exchange parameter, provided the *R* positions can be considered constant across the series. In the case of *R*Cd, the lanthanide contraction decreases the cubic lattice parameter *a* by less than 5% from Ce to Tm. In Fig. 9, we have plotted the normalized exchange parameter $\Gamma(R)/\Gamma(\mathrm{Gd})$ of *R*Cd and *R*Zn for the nuclear probes ^{111}Cd and ^{119}Sn as a function of the atomic number of the *R* constituent. $\Gamma(R)/\Gamma(\mathrm{Gd})$ was calculated from the values of B_{hf} listed in Table I, assuming that $\Phi(r)$ and the parameter *C* in Eq. (5) are constant across the *R* series.

Information on the *R* dependence of the exchange parameter can also be extracted from the variation of the order temperature T_C, since [20] $T_C \propto \Gamma^2(g-1)^2 J(J+1)$. Both $B_{hf}(R)$ and $T_C(R)$ lead to same trend of $\Gamma(R)/\Gamma(\mathrm{Gd})$: The exchange parameter of *RX*, *X* = Cd, Zn, shows a pronounced decrease from Ce to Er, independently of the nuclear probe.

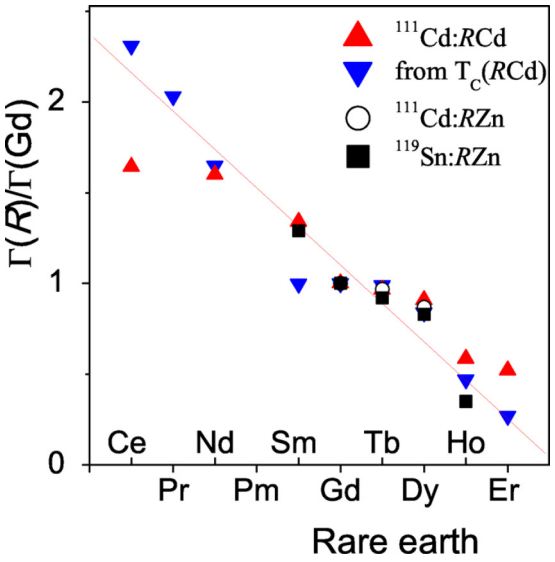

FIG. 9. The normalized coupling constant $\Gamma(R)/\Gamma(Gd)$ of the equiatomic rare-earth cadmium *R*Cd and rare-earth zinc compounds *R*Zn as a function of the rare-earth constituent, deduced from the hyperfine fields B_{hf} of ^{111}Cd (this work and Ref. [11]) and ^{119}Sn (Ref. [10]) and from the order temperatures of *R*Cd. The solid line is to guide the eye.

The same behavior observed in the series R_2In [36,38,39] has been related by Delyagin *et al.* [38,39] to differences in the radial extensions of the $4f$ and $5d$ electrons in the first and the second half of the *R* series. According to Delyagin *et al.* [38,39], the degree of $4f$-$5d$ overlap can be expressed by the ratio R_{4f}/R_{NN} where $R_{4f} = \langle r_{4f}^2 \rangle^{1/2}$ and the nearest-neighbor distance R_{NN} are measures of the radial extensions of the $4f$- and the $5d$-wave functions, respectively. In an isostructural series, both parameters decrease with increasing *Z*. The decrease of R_{NN} (lanthanide contraction) from Pr to Tm usually amounts to only a few percent. The $4f$ radius, however, shows a stronger *Z* dependence: it decreases about 20% in the first half and 10% in the second half of the *R* series. Consequently, the degree of overlap decreases from Pr to Tm, leading to weaker exchange in the second half of the *R* series.

The temperature dependence of B_{hf} of ^{111}Cd in most *R*Cd is rather well described by a molecular field model: The solid black lines in Figs. 3 and 7 are the Brillouin functions for the corresponding angular momenta *J*. The observation of a finite hyperfine field in SmCd at $T < 190$ K supports ferromagnetic order for this compound, in agreement with the result of Buschow [20]. The temperature dependence of $B_{hf}(T)$ of DyCd confirms the peculiar properties previously reported for this compound [18,20–22]: Anomalies in the magnetothermal curves of DyCd indicate the existence of two phase transitions, a first-order transition at $T \sim 40$ K and a second-order transition at $T \sim 79$ K. According to Aléonard and Morin [21,22], the magnetic ordering on both sides of the 40 K transition is ferromagnetic. Alfieri *et al.* [18] suggest a change in spin arrangement from ferromagnetic to a screw structure at $T \sim 40$ K. The interpretation of the 40 K transition by Buschow [40] involves chemical disorder caused by Dy atoms residing on Cd sites and vice versa. These crystal imperfections favor a local antiparallel arrangement of the magnetic moments. According to the present PAC study, the magnetic hyperfine field at ^{111}Cd in DyCd vanishes below $T \sim$ 35–40 K. This indicates a transition from ferromagnetic order to a spin arrangement where all $4f$-induced contributions to the magnetic hyperfine field at the Cd site cancel, such as a screw structure or antiferromagnetic arrangement.

TbCd presents a change of magnetic structure at $T =$ 67.5 K [21,22]. Upon cooling, the direction of easy magnetization changes from fourfold [110] to twofold [100]. This change coincides with the appearance of a finite quadrupole interaction in the PAC spectra of TbCd (Fig. 5) suggesting that the change of magnetic structure involves a distortion of the CsCl symmetry. It is interesting to note that in the case of NdCd where a change of direction from [111] to [100] occurs at $T \sim 63$ K, a quadrupole interaction was not found in the transition region.

First-principles calculations

In an attempt to explain the behavior of the temperature dependence of B_{hf} for DyCd we performed first-principles calculations simulating different configurations for the spin alignment of Dy atoms. Self-consistent calculations from density functional theory [41,42] have been performed using the WIEN2k computer code [43], in which the Kohn-Sham

equations in the crystal are solved with the utilization of a basis set consisting of augmented plane waves plus local orbitals (APW+lo) and applying an all-electron method. The muffin-tin sphere radius $R_{MT} = 2.5$ a.u. was chosen for the rare-earth and Cd atoms. The number of plane waves was limited by the cutoff $K_{max} = 7/R_{MT}^{min}$, and the charge density was Fourier expanded up to $G_{max} = 14$. For the Brillouin zone integrations, meshes of k points obeying the following rule were adopted: number of atoms times number of k points equals 30 000. Thus, for larger supercells, correspondingly smaller number of k points were utilized. Exchange and correlation effects were treated with the local density approximation (LDA) which is parametrized by Perdew-Wang [44]. Calculations were performed taking into account the spin polarization and the core states are relaxed in a fully relativistic manner. A supercell was used to simulate the antiferromagnetism in DyCd. These supercells were built up from a $\sqrt{2} \times \sqrt{2} \times 1$ [$1 \times 1 \times 2$ for $(0, 0, \pi)$ configuration] DyCd single cell with a total of four atoms (two of each element).

We have simulated three different configurations for the antiferromagnetic supercell: the $(0, 0, \pi)$, $(\pi, \pi, 0)$, and (π, π, π) magnetic structure as well as that for a ferromagnetic structure. Results for the total energy as a function of the cell volume for each simulation are displayed in Fig. 10. Since the magnetic supercells have a different number of atoms for each configuration, all energy values were normalized for the ferromagnetic unit cell volume. The absolute energy does not have physical meaning, only differences do. The lowest energy for each configuration occurs at a volume which is 6% smaller than that of the experimental volume, which is a known feature of the LDA approximation. Results show that the curve with the lowest energy is that for the $(\pi, \pi, 0)$ antiferromagnetic configuration and that the next lowest energy corresponds to the ferromagnetic curve. The difference

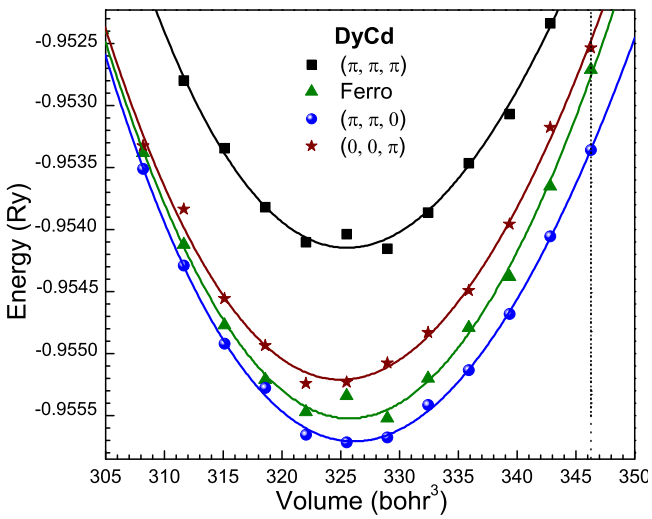

FIG. 10. Normalized total energy of the unit cell as a function of cell volume for different magnetic structures of DyCd simulated by first-principles calculations. Each symbol in the figure corresponds to a volume step 1% of experimental volume (represented by the vertical dotted line). The minimum in energy occurs at −6% (325.5 bohr^3). Lines are the Murnaghan [45] fits.

in energy between these two configurations is 2.72 meV at the volume corresponding to the lowest energy of each curve. This value corresponds to 32 K, which is quite close to the temperature for which the B_{hf} vanishes as observed from the experimental measurements (see Fig. 7). We, therefore, propose that the observed behavior for the B_{hf} at Cd sites in DyCd is due to a first-order transition from ferromagnetic to antiferromagnetic ordering at around 35 K when temperature decreases.

Another possible situation where B_{hf} at Cd sites could vanish is a chemical disorder with Dy atoms at Cd sites and vice versa. To inspect this possibility we performed calculations to simulate such a disorder for some situations of a ferromagnetic cell: without exchange of atoms, one exchange where one Cd and one Dy atom exchange positions, two exchanges where two Cd and two Dy atoms exchange positions, three exchanges where three Cd and three Dy atoms exchange positions, and four exchanges where four Cd and four Dy atoms exchange positions. Because of the cubic symmetry of the compound, the replacement of five Dy would repeat the first configuration and so on. In all these situations, B_{hf} at Cd sites does not vanish. In simulations where there is chemical disorder B_{hf} does not vanish but its value (∼6–13 T) is smaller than that for the situation without disorder for which $B_{hf} = 18$ T. This value is very close to the experimental value of 20 T extrapolated to 0 K from PAC measurements at the ferromagnetic region. This agreement is a very good indication that first-principles calculations correctly simulated the magnetic ordering in the DyCd compound. Moreover, the fact that experimental measurements have not observed B_{hf} values around 6–13 T (predicted by calculations for chemical disorder) also reinforces the conclusion that disorder is not responsible for the magnetic transition in DyCd. Furthermore, as disorder means a break of the symmetry, a high degree of disorder would produce a nonvanishing nuclear quadrupole interaction, which is not observed by experiment (see result at 80 K in Fig. 5).

The same method of calculation was used to simulate the ferromagnetic ordering in other compounds of the *R*Cd family in order to compare the results with experimental values of B_{hf} measured with PAC spectroscopy and extrapolated to 0 K. Results from calculations are shown in Table II, where values of valence and core contributions to the calculated B_{hf} are given. As we are focusing on calculating the magnetic hyperfine field at Cd sites in a series of compounds with different rare-earth elements, we have avoided the use of the DFT+U approach since the Hubbard parameter U value is arbitrarily chosen and, probably, different U values might be used for each studied compound. Moreover, a significant change in the B_{hf} at Cd sites is not expected because the LDA+U approach will affect the electronic configuration in the rare-earth ion with a change in the localized magnetic moment [46]. Nevertheless, we have tested the LDA+U approach with $U_{eff} = 0.55$ Ry [47] taking into account the spin-orbit interaction to simulate the ferromagnetic configuration in TbCd and DyCd, as well as the possible different antiferromagnetic configurations of DyCd. Results show no significant differences from those obtained with LDA. B_{hf} for TbCd and DyCd in the ferromagnetic configuration calculated with LDA+U are, respectively, −27.98 T and −22.19 T.

TABLE II. Theoretical values for valence (B_{hf}^{val}) and core (B_{hf}^{core}) contributions to the total magnetic hyperfine field (B_{hf}^{total}) determined by first-principles calculations. B_{hf}^{val} was calculated from Cd-5*s* and *R*-6*s* electrons and B_{hf}^{core} from Cd-1 *s*, -2 *s*, -3 *s*, and -4*s* electrons. The saturation value of the experimental magnetic hyperfine field $B_{hf}^{exp}(0)$ at ^{111}Cd in *R*Cd extrapolated to 0 K from the low-temperature PAC spectra is also shown.

	Theoretical results			
Compound	B_{hf}^{val} (*T*)	B_{hf}^{core} (*T*)	B_{hf}^{total} (*T*)	$B_{hf}^{exp}(0)$ (*T*)
CeCd	− 5.61	− 0.14	− 5.75	5.10
PrCd	− 13.65	− 0.27	− 13.92	
NdCd	− 15.69	− 0.20	− 15.89	17.4
SmCd	− 21.80	− 0.18	− 21.98	21.1
GdCd	− 34.78	− 0.33	− 35.11	30.8
TbCd	− 25.53	− 0.14	− 25.67	25.6
DyCd	− 17.86	− 0.05	− 17.91	20.0
HoCd I	− 11.73	− 0.01	− 11.74	10.3
HoCd II	− 11.73	− 0.01	− 11.74	10.3
ErCd	− 6.27	0.05	− 6.22	6.9

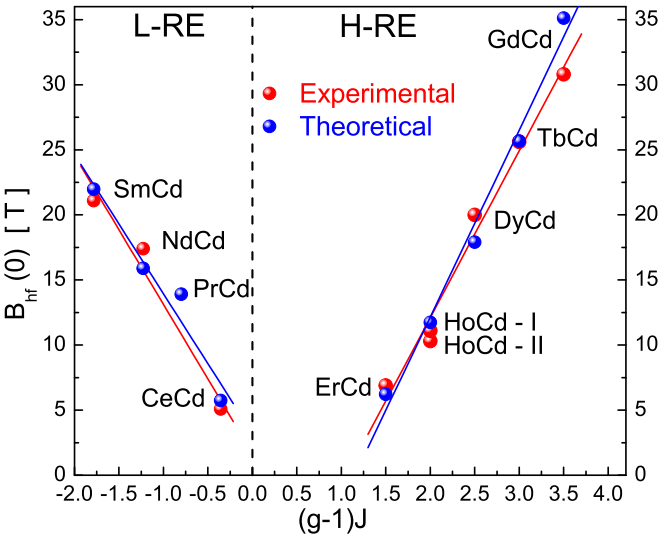

FIG. 11. Spin dependence of experimental and theoretical saturation values of B_{hf} at 0 K. Straight lines are the linear fit to the values.

In addition, the LDA+U calculations also show that the ground state (at 0 K) of DyCd corresponds to the (π, π, 0) antiferromagnetic configuration. Results of calculations for B_{hf} at Cd atoms, therefore, do not depend on the interaction between 4*f* electrons in the neighboring *R* atoms, taking into account by the DFT+U approximation. Similar conclusions have been reported previously. Mohanta *et al.* [48] have reported that results of calculations using GGA and GGA+U of B_{hf} at Cd impurity in rare-earth metals do not appreciably differ from each other. Richard *et al.* [49] have concluded that in calculations using LSDA the application of the U correction to 4*f* bands in rare-earth oxides does not significantly affect the electric field gradient at Cd impurity sites.

Figure 11 displays a comparison of experimental (extrapolated to 0 K) and calculated $B_{hf}(0)$ as a function of the spin projection $(g-1)J$ on the total angular momentum J of the *R* ion. The agreement between experimental and theoretical values is very good for the entire series of compounds (the difference is at maximum 13%). The good agreement between calculated and experimental values of B_{hf} is not expected and it is unusual for methods based on DFT. DFT calculations are known to give wrong values for the core contribution [48,50,51]. We believe that the good agreement was achieved because two conditions were fulfilled: first, Cd atoms have a closed shell and the B_{hf}^{c} contribution is very small compared with the contribution from valence, and second, Cd is not an impurity but it is a constituent atom of the compound; i.e., it was not necessary to add an impurity atom to simulate the PAC probe nuclei, as usual in compounds where Cd is not the native atom.

B. Critical increase of the magnetic linewidth near T_C

The PAC spectra of all magnetic *R*Cd compounds investigated here show a pronounced loss of oscillation amplitude as temperature approaches the order temperature T_C. An attenuation of the magnetic precession amplitudes occurs when the magnetic hyperfine field presents a distribution of relative width δ rather than a unique, sharply defined value. The increase of the attenuation then implies a critical increase of the linewidth near T_C. A similar observation has been made in practically all investigations of magnetic hyperfine fields in chemically ordered intermetallic compounds reported up to now. The PAC spectra of ^{111}Cd:RCo_2 [52], ^{111}Cd:R_2In [36], ^{181}Ta:RFe_2 [53], and ^{181}Ta:$ZrFe_2$ [54] all show an extreme attenuation—in most cases even the total destruction—of the magnetic precession pattern near T_C.

Such a behavior can be understood as evidence for a distribution of the order temperature which has first been found in disordered ferromagnetic systems. T_C spreads of the order of a few K, resulting in critical line broadening and phase coexistence near T_C, have been observed by Moessbauer [55,56] and PAC [57] spectroscopy in concentrated and dilute disordered alloys. The quoted PAC studies [36,52–54] show that distributions of the order temperature may also occur in chemically ordered intermetallic compounds, possibly due local chemical disorder. A T_C distribution produces a critical increase of the linewidth, in particular at second-order transitions (SOTs), because at low temperatures the magnetic frequency ν_m varies little with the Curie temperature, but close to T_C the frequency ν_m decreases critically with increasing T: $\nu_m(T) = \nu_m(0)(1 - T/T_C)^{\beta}$ with an exponent of the order $\beta \sim 0.3$–0.4 [58]. At $T \approx T_C$, small variations of the Curie temperature therefore produce broad distributions of ν_m, while at low T the magnetic frequency remains sharply defined. As shown in detail in Ref. [52], for a SOT with critical exponent β and a Lorentzian T_C distribution, characterized by the center temperature T_{C0} and the width Γ_C, the resulting temperature dependence of the relative linewidth δ is given by

$$\delta(T, T_{C0}) = \frac{\Delta\nu_m(T, T_{C0})}{\nu_m(T, T_{C0})} \approx \frac{\beta\Gamma_C}{T_{C0}} \frac{T}{T_{C0}} \left(1 - \frac{T}{T_{C0}}\right)^{-1}. \quad (6)$$

Fits of Eq. (6) to the experimental data in Figs. 3 and 7 (red solid lines) provide a very close description of the critical increase of the relative linewidth δ towards T_C and thus strongly suggest the existence of relatively broad distributions of the order temperature in the *R*Cd compounds investigated here. With $\beta = 1/3$, the fits give linewidths Γ of the T_C distribution ranging from $\Gamma \sim 7$ K for DyCd to $\Gamma \sim 15$ K for SmCd. These values reflect a high concentration of lattice imperfections resulting in spatial distribution of the order temperature. Perturbations of the crystal symmetry by chemical disorder, i.e., *R* atoms occupying Cd sites and vice versa, have been invoked by Buschow [40] to explain the special magnetic properties of the compounds DyCd.

V. SUMMARY

Perturbed angular correlation (PAC) spectroscopy has been used to investigate the magnetic hyperfine field B_{hf} of the nuclear probe ^{111}In/^{111}Cd in the rare-earth (*R*) cadmium intermetallic compounds *R*Cd and $GdCd_2$. The observation that the hyperfine parameters depend on details of the sample preparation provides information on the phase preference of diffusing ^{111}In in the rare-earth cadmium phase system.

In cubic CsCl-type compounds *R*Cd the hyperfine field was determined for the *R* constituents Ce, Pr, Nd, Sm, Gd, Tb, Dy, Ho, Er, mostly as a function of temperature. The variation of the ^{111}Cd hyperfine field of *R*Cd and of the magnetic order temperature with the *R* constituent indicates a decrease of the indirect $4f$-$4f$ exchange with increasing *R* atomic number. For most *R* constituents, the temperature dependence $B_{hf}(T)$ of ^{111}Cd:*R*Cd is consistent with ferromagnetic order of the compound. DyCd, however, presents a remarkable anomaly with phase transitions at $T \sim 35$ K and 80 K, respectively. The disappearance of the hyperfine field below 35 K is attributed to a spin arrangement where all $4f$-induced contributions to the magnetic hyperfine field at the Cd site cancel. First-principles calculations show that the antiferromagnetic configuration of spins in DyCd is energetically more favorable than the ferromagnetic, resulting in a zero value for B_{hf} at Cd. The PAC spectra reflect a distribution rather than a unique value of the magnetic hyperfine interaction. The critical increase of the distribution width towards the magnetic-order temperature can be attributed to a distribution of the order probably due chemical disorder of the *R* and Cd sublattices.

ACKNOWLEDGMENTS

F.H.M.C. gratefully acknowledges the funding of this research by a Fundação de Amparo à Pesquisa do Estado de São Paulo (FAPESP, Brazil) through Grants No. 2011/14097-0 and No. 2012/11104-9 fellowship. A.W.C. and R.N.S. gratefully acknowledge the support provided by Conselho Nacional de Desenvolvimento Científico e Tecnológico (CNPq, Brazil) in the form of research fellowships. M.F. expresses his thanks for the kind hospitality extended to him at CBPF and the financial support by CAPES and FAPERJ (Brazil).

[1] R. G. Barnes, in *Handbook of Chemistry and Physics of Rare Earths*, edited by K. A. Gschneidner and L. Eyring (North-Holland, Amsterdam, 1979), Vol. 2, Chap. 18.
[2] I. Iandelli and A. Palenzona, in *Handbook of Chemistry and Physics of Rare Earths*, edited by K. A. Gschneidner and L. Eyring (North-Holland, Amsterdam, 1979), Vol. 2, Chap. 13.
[3] K. H. J. Buschow, Rep. Prog. Phys. **42**, 1373 (1979).
[4] M. Forker, Hyperfine Interact. **24-26**, 907 (1985).
[5] P. Morin, *Compounds of Rare Earth Elements with Main Group Elements, Part 2*, edited by H. P. J. Wijn, Landolt-Börnstein, New Series, Group III, Vol. 19e2 (Springer, Berlin, 1989), pp. 22–36.
[6] Y. Kasamatsu, K. Kojima, and T. Hihara, J. Phys. Soc. Jpn. **63**, 1508 (1994).
[7] Y. Kasamatsu, K. Kojima, and T. Hihara, J. Magn. Magn. Mater. **140-144**, 1149 (1995).
[8] Y. Kasamatsu, T. Tohyama, K. Kojima, and T. Hihara, J. Magn. Magn. Mater. **70**, 294 (1987).
[9] A. L. de Oliveira, M. V. Tovar Costa, N. A. de Oliveira, and A. Troper, J. Appl. Phys. **87**, 4882 (2000).
[10] S. I. Reiman and I. N. Rozantsev, Zh. Eksp. Teor. Fiz. **102**, 704 (1992) [Sov. Phys. JETP **75**, 378 (1992)].
[11] B. Bosch-Santos, A. W. Carbonari, G. A. Cabrera-Pasca, M. S. Costa, and R. N. Saxena, J. Appl. Phys. **113**, 17E136 (2013).
[12] B. Bosch-Santos, A. W. Carbonari, G. A. Cabrera-Pasca, M. S. Costa, and R. N. Saxena, Hyperfine Interact. **221**, 59 (2013).
[13] B. Bosch-Santos, G. A. Cabrera-Pasca, A. W. Carbonari, M. S. Costa, and R. N. Saxena, in Proceedings of the International Nuclear Atlantic Conference - INAC 2011, held in Belo Horizonte, MG, Brazil, October 24-28, 2011.
[14] A. Iandelli and A. Palenzona, J. Less-Common Met. **15**, 273 (1968).
[15] G. Bruzzone, M. L. Fornasini, and F. Merlo, J. Less-Common Met. **25**, 295 (1971).
[16] A. M. Mulokozi, J. Less-Common Met. **53**, 205 (1977).
[17] N. Fujita, S. Kikuchi, and A. Tsai, Solid State Sci. **13**, 698 (2011).
[18] G. T. Alfieri, E. Banks, K. Kanematsu, and T. Ohoyama, J. Phys. Soc. Jpn. **23**, 507 (1967).
[19] M. Nakazato, N. Wakabayashi, and T. Kitai, J. Phys. Soc. Jpn. **57**, 953 (1988).
[20] K. H. J. Buschow, J. Chem. Phys. **61**, 4666 (1974).
[21] R. Aléonard and P. Morin, J. Magn. Magn. Mater. **50**, 128 (1985).
[22] R. Aléonard and P. Morin, J. Magn. Magn. Mater. **42**, 151 (1984).
[23] R. P. Pinto, M. M. Amado, M. E. Braga, J. B. Sousa, P. Morin, and R. Al'eonard, J. Magn. Magn. Mater. **72**, 152 (1988).
[24] R. Aléonard and P. Morin, Solid State Commun. **56**, 627 (1985).
[25] H. Fujii, T. Kitai, Y. Uwatoko, and T. Okamoto, J. Magn. Magn. Mater. **52**, 428 (1985).
[26] T. Kitai, H. Fujii, T. Okamoto, and Y. Hashimoto, Solid State Commun. **52**, 407 (1984).
[27] M. A. Ruderman and C. Kittel, Phys. Rev. **96**, 99 (1954); T. Kasuya, Prog. Theor. Phys. **16**, 45 (1956); K. Yosida, Phys. Rev. **106**, 893 (1957).
[28] A. I. Goldman, T. Kong, A. Kreyssig, A. Jesche, M. Ramazanoglu, K. W. Dennis, S. L. Bud'ko, and P. C. Canfield, Nat. Mater. **12**, 714 (2013).

[29] H. Frauenfelder and R. M. Steffen in *Perturbed Angular Correlations*, edited by K. Karlsson, E. Matthias, and K. Siegbahn (North-Holland, Amsterdam, 1964), Chap. I.
[30] L. Boström, E. Karlsson, and S. Zetterlund, Phys. Scr. **2**, 65 (1970).
[31] T. Kitai, J. Phys. Soc. Jpn. **64**, 3403 (1995).
[32] F. H. M. Cavalcante, L. F. D. Pereira, H. Saitovitch, J. Mestnik-Filho, A. F. Pasquevich, and M. Forker, Hyperfine Interact. **221**, 123 (2013).
[33] F. H. M. Cavalcante, L. F. D. Pereira, J. T. Cavalcante, H. Saitovitch, A. W. Carbonari, R. N. Saxena, and M. Forker, J. Appl. Phys. **113**, 17E139 (2013).
[34] E. N. Kaufmann and R. J. Vianden, Rev. Mod. Phys. **51**, 161 (1979).
[35] I. A. Campbell, J. Phys. F: Met. Phys. **2**, L47 (1972).
[36] M. Forker, R. Müsseler, S. C. Bedi, M. Olzon-Dionysio, and S. D. de Souza, Phys. Rev. B **71**, 094404 (2005).
[37] E. Daniel and J. Friedel, J. Phys. Chem. Solids **24**, 1601 (1963).
[38] N. N. Delyagin, G. T. Mudzhiri, V. I. Nesterov, and S. I. Reiman, Zh. Eksp. Teor. Fiz. **86**, 1016 (1984) [Sov. Phys. JETP **59**, 592 (1984)].
[39] N. N. Delyagin, G. T. Mujiri, and V. I. Nesterov, Zh. Eksp. Teor. Fiz. **96**, 1896 (1989) [Sov. Phys. JETP **69**, 1070 (1989)].
[40] K. H. J. Buschow, J. Appl. Phys. **44**, 1817 (1973).
[41] P. Hohenberg and W. Kohn, Phys. Rev. **136**, B864 (1964).
[42] W. Kohn and L. J. Sham, Phys. Rev. **140**, A1133 (1965).
[43] P. Blaha, K. Schwarz, G. Madsen, D. Kvasnicka, and J. Luitz, *WIEN2k: An Augmented Plane Wave Plus Local Orbitals Program for Calculating Crystal Properties* (Technische Universität Wien, Austria, 2001).
[44] J. P. Perdew and Y. Wang, Phys. Rev. B **45**, 13244 (1992).
[45] F. D. Murnaghan, Proc. Natl. Acad. Sci. USA **30**, 244 (1944).
[46] J. L. F. Da Silva, M. V. Ganduglia-Pirovano, J. Sauer, V. Bayer, and G. Kresse, Phys. Rev. B **75**, 045121 (2007).
[47] J. Mestnik-Filho, L. F. D. Pereira, M. V. Lalić, and A. W. Carbonari, Physica B **389**, 73 (2007).
[48] S. K. Mohanta, S. N. Misha, S. K. Srivastava, and M. Rots, Solid State Commun. **150**, 1789 (2010).
[49] D. Richard, E. L. Muñoz, M. Renteria, L. A. Errico, A. Svane, and N. E. Christensen, Phys. Rev. B **88**, 165206 (2013).
[50] P. Novák, J. Kuneš, W. E. Pickett, Wei Ku, and F. R. Wagner, Phys. Rev. B **67**, 140403(R) (2003).
[51] M. V. Lalić, J. Mestnik-Filho, A. W. Carbonari, R. N. Saxena, and H. Haas, Phys. Rev. B **65**, 054405 (2001).
[52] M. Forker, S. Müller, P. de la Presa, and A. F. Pasquevich, Phys. Rev. B **68**, 014409 (2003).
[53] B. A. Komissarova, G. K. Ryasny, L. G. Shnipkova, A. A. Sorokin, A. V. Tavyashchenko, L. M. Fomichova, and A. S. Denisova, Aust. J. Phys. **51**, 175 (1998).
[54] A. T. Motta, G. L. Catchen, S. E. Cumblidge, R. L. Rasera, A. Paesano, and L. Amaral, Phys. Rev. B **60**, 1188 (1999).
[55] G. S. Collins, A. R. Chowdhury, and C. Hohenemser, Phys. Rev. B **26**, 4997 (1982).
[56] X. S. Chang, C. Hohenemser, and L. Takacs, Phys. Rev. B **40**, 29 (1989).
[57] R. M. Suter and C. Hohenemser, in *Magnetism and Magnetic Materials 1975*, edited by J. J. Becker, G. H. Lander, and J. J. Rhyne, AIP Conf. Proc. No. 29 (AIP, New York, 1976), p. 493.
[58] C. Hohenemser, N. Rosov, and A. Kleinhammes, Hyperfine Interact. **49**, 267 (1989).